A Model for Gas-Liquid Slug Flow at Reduced Gravity Conditions

Antoine Janicot and Abraham E. Dukler
Chemical Engineering Dept., University of Houston, Houston, TX 77204

The gas-liquid slug flow pattern exists over a broad range of flow rate space at reduced gravity conditions and for that reason is expected to be widespread in many space applications. The objective of this work was to develop a model predicting the characteristics of slug flow at reduced gravity including the bubble length, shape, velocity and other properties of the slug flow. Observations derived from low-gravity experiments suggested the use of a boundary layer-type approach. Multiple solutions exist, and a criterion for selecting the solution which corresponds to experimental observation is indicated.

Introduction

Two-phase gas-liquid flow is expected to occur in a wide variety of applications in space. Low-gravity trajectories carried out on a Learjet executing parabolic trajectories show that three flow patterns can exist: bubble, annular and slug flows. A description of these patterns and the analysis of the conditions for their existence have been presented by Dukler et al. (1988) and Janicot (1988).

During slug flow, most of the gas is located in large bullet-shaped "Taylor" bubbles which have a diameter almost equal to the pipe diameter. The Taylor bubbles are separated by slugs of continuous liquid which bridge the pipe and can contain smaller bubbles. This is shown in Figure 1 which is an enlarged copy of a single frame taken from a 400 frames per second movie film of slug flow (Janicot, 1988). In this run, the tube diameter was 0.0127 m, gravity level was less than 0.02 g, and the flow was filmed at a location 97 diameters downstream of the entry. The intermittent nature of the flow, as the large gas bubbles and liquid slugs propagate downstream, results in a complex pattern of oscillations in the measured pressure drop and void fraction. These oscillations can impose fluctuations in force on the confining piping as well as time variations in rates of heat transfer.

At normal gravity conditions, Dumitrescu (1943) initiated a line of studies considering the potential flow around a Taylor bubble in the absence of viscous effects. Davies and Taylor (1950), Collins et al. (1978), and Bendiksen (1985) contributed also to this class of problem with more experimental and theoretical work. In contrast, an approach based on the creeping flow premise, where the inertia forces are neglected, was introduced by Bretherton (1969) and elaborated by Reinelt (1987). A similar solution for very low Reynolds numbers was proposed by Coney and Massica (1969) at reduced gravity conditions. An analysis for the vertical tube at normal gravity, were both viscous and inertia effects are included, was proposed by Mao and Dukler (1990). The shape of the Taylor bubble, along with its propagation velocity and the flow field in the surrounding fluid, was computed using a finite difference technique. The lengthy code which was developed requires large amounts of computer time and limits the ability to examine a variety of cases of interest. It is the intention of this work to present a simple model that includes the viscous and inertia terms using the concept of the boundary layer to model slug flow at reduced gravity conditions.

Physical Model

Movie films from 42 experimental runs were studied in which slug flow existed at reduced gravity levels less than 0.02 g. In these runs, superficial liquid velocities ranged from 0.03 to 1 m/s with gas superficial velocities ranging from 0.05 to 2 m/s (Janicot, 1988). These runs show that, once slug flow is

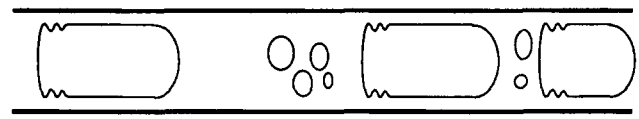

Figure 1. Continuous slug flow.

Correspondence concerning this article should be addressed to A. E. Dukler.

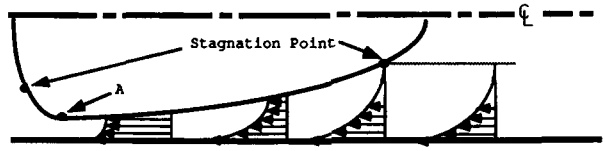

Figure 2. Boundary layer during slug flow in a moving coordinate system.

established, the large bubbles and liquid slugs all move with remarkably constant velocity in the axial direction with no overtaking. Furthermore, the small bubbles in the liquid slugs appear to be located in the central region of the liquid slug and travel at precisely the same velocity as the large bubble. That is, in a coordinate system fixed on the front of a large bubble they appear stationary. Since there is no gravity-induced slip, one can conclude that the liquid surrounding the bubbles is also at rest in the moving coordinate system. For the 12–20 slugs observed during each reduced gravity run, measured propagation velocities varied by less than 4%, well within measuring accuracy. This result is very different from that which occurs at 1 g (Mao and Dukler, 1988), where the standard deviation in slug velocity is about 35 percent of the mean and where the small bubbles in the liquid slug drift backward relative to the nose of the large bubble indicating a backward flow of liquid relative to the nose.

These observations suggest that at reduced gravity the flow is controlled by the liquid motion in the small region close to the pipe wall for both the large bubble and the liquid slug. The notion of a thin layer close to a solid wall, where the viscous effects are important and where they are comparable in magnitude to the inertial forces suggests the use of a boundary layer approach to the modeling problem. Figure 2 shows the lower half of an axisymmetrical bubble in the pipe showing the development of the boundary layer in the liquid film between the Taylor bubble and the pipe wall. This receding liquid film forms the boundary layer having a zero shear stress at the interface but with no constraint on the interfacial velocity. The boundary layer must end at points on the gas-liquid interface, where the local velocity is equal to the propagation velocity of the bubble. In a coordinate system moving with the bubble velocity, U_o, this matching takes place at stagnation points on the bubble interface. These stagnation points are located very close to the wall, and the placement in Figure 2 is for the clarity of illustration only.

At 1 g, many investigators (Dumitrescu, 1943; Davies and Taylor, 1950; Mao and Dukler, 1990) have shown that the nose of a Taylor bubble behaves as if it moves through an inviscid fluid. In the absence of shear stresses, surface tension forces cause the nose region to assume a spherical shape having constant mean curvature. As discussed above, the observations from experiment suggest that the liquid between the axis and the ring of stagnation points at both the rear and front surfaces of the bubble is at rest (in the moving coordinate system). Thus, we assume that surface tension, in the absence of viscous stresses, causes the mean curvature between the axisymmetrically located stagnation points at the front to be constant. Stagnation points also exist on the rear surface of the bubble; the curvature there is also assumed to be constant, although not necessarily having the same magnitude as at the front. This condition provides a method to select the velocity of a Taylor bubble from the infinity of such velocities which satisfy the equations of motion and boundary conditions.

To check the suitability of the boundary layer hypothesis, the shape of a typical Taylor bubble was measured during a reduced gravity run and the flow field computed with the finite difference algorithm of Mao and Dukler (1990). This computation developed the complete velocity and pressure field. It showed that there exists a thin layer close to the pipe wall where the velocity goes from zero at the wall to the velocity at the interface and across which the pressure is essentially constant, thus justifying the use of the boundary layer approach.

The boundary layer equations were solved with an integral method using a second-order polynomial velocity profile. The problem was constructed in a coordinate system moving with the Taylor bubble velocity, U_o. In the liquid film around the bubble, the coefficients of the polynomial can be expressed in terms of the local film thickness using the boundary conditions at the wall along with the normal pressure conditions (related to the curvature at the interface) and the zero shear stress at the interface. The bubble is a region of constant pressure. The result of these operations is a third-order differential equation which can be solved for the film thickness surrounding the bubble as a function of position along the bubble. It is necessary to assume a starting condition, and this important step in the process is described below.

In addition to the shape of the Taylor bubble and the thickness of the liquid film around it, the model predicts the length of the liquid slug once information is available on the slug frequency and slug void fraction. At 1 g, the frequency has been shown to be determined by the process of slug formation in the entry region or the mixing device (Taitel and Dukler, 1977; Tronconi, 1990). Measurements by Janicot (1988) show that slug frequencies are essentially unchanged along the length of the 0.0127-m-ID tube suggesting that the mixing device at the entry controls the frequency. In applying the method described here, the slug frequency and void fraction are obtained from experimental data. Given flow rates, slug frequency, void fraction, and tube diameter, the model presented here makes it possible to calculate the propagation velocity, U_o, the length and shape of the Taylor bubble, and the length of the liquid slug.

Overall Mass-Balance Relationships

The equations derived assume that fully developed and stable slug flow exists. The overall mass-balance relationships are derived from the same procedure used for vertical flows by Fernandes et al. (1983). Figure 3 identifies the variables of interest.

U_S = liquid velocity in the slug
U_G = gas velocity in the liquid slug
U_f = liquid velocity in film surrounding the Taylor bubble
U_B = gas velocity in the Taylor bubble
U_O = propagation velocity of the Taylor bubble
U_{SG} = superficial gas velocity
U_{SL} = superficial liquid velocity
U_m = superficial mixture velocity, $U_{SL}+U_{SG}$
L_B = Taylor bubble length
L_S = slug length
α_B = void fraction over length of the Taylor bubble
α_S = void fraction in the liquid slug
α_{SU} = void fraction of the slug unit
β = $L_B/(L_S+L_B)$

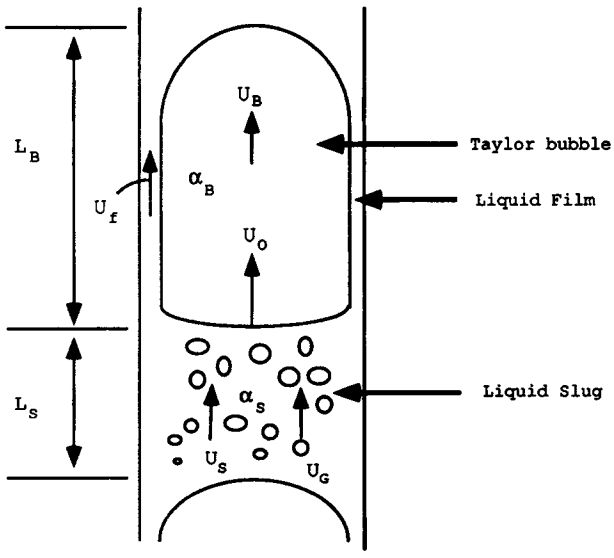

Figure 3. Typical slug flow unit.

Velocities and void fractions represent values averaged over flow areas.

For fluids of constant density, the material balances over slug and Taylor bubbles are:

$$\alpha_S U_S + (1+\alpha_S) U_G = U_m \tag{1}$$

$$\alpha_B U_B + (1-\alpha_B) U_f = U_m \tag{2}$$

An independent continuity relationship can be found by taking a balance in a coordinate system fixed on the nose of the bubble:

$$U_{DL} = (1-\alpha_S)(U_O - U_S) = (1-\alpha_B)(U_O - U_f) \tag{3}$$

$$U_{DG} = \alpha_s (U_O - U_G) = \alpha_B (U_O - U_B) \tag{4}$$

where U_{DL} and U_{DG} are known as "drift" velocities.

Liquid and gas superficial velocities, U_{SL} and U_{SG} are related to the drift velocities as follows:

$$U_{SL} = (1-\alpha_{SU}) U_O - U_{DL} \tag{5}$$

$$U_{SG} = \alpha_{SU} U_O - U_{DG} \tag{6}$$

The void fraction of a slug unit consisting of a liquid slug plus its trailing bubble is:

$$\alpha_{SU} = (1-\beta)\alpha_S + \beta \alpha_B \tag{7}$$

Studies of movie films taken during slug flow showed that the gas bubbles in the liquid slug and the Taylor bubble move at the same velocity as discussed earlier. Therefore, the drift velocity, $U_{DG} = 0$. The material balance equations then reduce to:

$$U_S = U_m \tag{8}$$

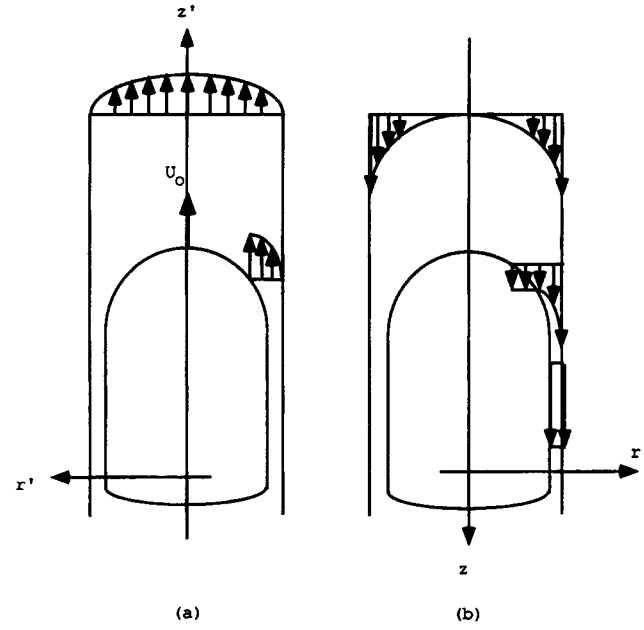

Figure 4. Slug flow in fixed (a) and moving (b) coordinate systems.

$$U_G = U_B = U_O \tag{9}$$

$$\alpha_{SU} = (1-\beta)\alpha_S + \beta \alpha_B \tag{10}$$

$$U_G = \alpha_{SU} U_O \tag{11}$$

$$U_S = U_G \tag{12}$$

Integral Momentum and Mass-Balance Equations

Consider a Taylor bubble moving at a velocity U_O relative to the tube wall (Figure 4a). This unsteady problem becomes a steady one when viewed in a coordinate system moving with the bubble (Figure 4b). Since the flow is axisymmetric, we use the Navier-Stokes equation in cylindrical coordinates to describe the flow around the bubble. The boundary layer approach suggests that gradients of velocity exist only in the regions near the wall, and the pressure is independent of the radial position. These assumptions lead to:

$$\frac{\partial u}{\partial z} + v\frac{\partial u}{\partial r} = -\frac{1}{\rho}\frac{\partial p}{\partial z} + \nu\left[\frac{1}{r}\frac{\partial}{\partial r}\left(r\frac{\partial u}{\partial r}\right) + \frac{\partial^2 u}{\partial^2 z}\right], \tag{12}$$

where u and v are the local velocities in the z and r directions expressed in the moving coordinate system.

To solve this boundary-layer-type equations, we use the integral technique where the momentum equation is integrated over the coordinate normal to the flow. The limits of the integration are $R-h$ and R, where h is the boundary layer film thickness. The resulting integral momentum equation is:

$$\frac{d}{dz}\left(\int_{R-h}^{R} r u^2 dr\right) = \nu R\left[\frac{\partial u}{\partial r}\right]_w - \frac{[R^2-(R-h)^2]}{2\rho}\frac{dp}{dz} \tag{13}$$

Boundary conditions at the interface can be specified by recognizing that the low density and viscosity of the gas within the Taylor bubble result in a constant pressure, p_o, there and negligible interfacial shear. These conditions have been shown to exist at 1 g (Fernandes et al., 1983). The difference in normal stress across the gas-liquid interface is then controlled by the curvature of the surface and surface tension. As a result, the following boundary conditions apply at the gas-liquid interface (Mao and Dukler, 1990):

$$\left[p = p_o - \sigma\left(\frac{1}{R_1} + \frac{1}{R_2}\right)\right]_i \tag{14}$$

$$\left[\frac{\partial u}{\partial r}\right]_i = 0 \tag{15}$$

where i represents a quantity estimated at the gas-liquid interface, and R_1 and R_2 are the local radii of curvature related to h and its derivatives given by:

$$\frac{1}{R_1} + \frac{1}{R_2} = \frac{\left(\frac{d^2h}{dz^2}\right)}{\left[1 + \left(\frac{dh}{dz}\right)^2\right]^{3/2}} + \frac{1}{(1-h)\left[1 + \left(\frac{dh}{dz}\right)^2\right]^{1/2}} \tag{16}$$

Computations have shown that the viscous stresses which have been neglected in Eqs. 14 and 15 are indeed negligible at all locations along the surface up to the stagnation point.

In the moving coordinate system (Figure 4b), the liquid flow rate is constant in the axial direction so that the flow rate through the film can be equated to that flowing in the slug. Thus, the mass balance for the liquid having constant density becomes:

$$2\int_{R-h}^{R} rudr = [U_0 - U_m]R^2(1-\alpha_S) \tag{17}$$

The smallest possible film thickness, h_o, exists for a very long bubble such that the liquid in the film would come to rest in a fixed coordinate system as a result of wall shear. For this condition, the film would assume a velocity, U_o, in the moving coordinate system. Thus, h_o can be found from the mass balance between the flow in the slug and in the film which in the moving coordinate system achieves a uniform velocity of U_o:

$$[U_o - U_m]R^2(1-\alpha_S) = U_O[R^2 - (R-h_o)^2] \tag{18}$$

h_o is useful in setting the lower limit for h in the integrations which are discussed below.

A dimensionless form of the equations can be developed by substituting the following normalized variables:

$$\phi = \frac{u}{U_o},\ \delta = \frac{h}{R},\ \zeta = \frac{z}{R},\ \lambda = \frac{p - p_o}{\rho U_o^2},\ \eta = \frac{R-r}{h},\ \theta = \frac{U_m}{U_o} \tag{19}$$

Equations 13, 14, 15 and 17 then become:

$$Re\frac{d}{d\zeta}\left(\int_0^1 \delta(1-\delta\eta)\phi^2 d\eta\right) = -\frac{1}{\delta}\left[\frac{\partial\phi}{\partial\eta}\right]_w - Re\frac{[1-(1-\delta)^2]}{2}\frac{d\lambda}{d\zeta}, \tag{20}$$

$$2\int_0^{1-\delta} \delta(1-\delta\eta)\phi d\eta = (1-\theta)(1-\alpha_s) \tag{21}$$

$$\lambda = -\frac{1}{We}\left[\frac{\left(\frac{d^2\delta}{d\zeta^2}\right)}{\left(1 + \left(\frac{d\delta}{d\zeta}\right)^2\right)^{3/2}} + \frac{1}{(1-\delta)\left(1 + \left(\frac{d\delta}{d\zeta}\right)^2\right)^{1/2}}\right] \tag{22}$$

$$\left[\frac{\partial\phi}{\partial\eta}\right]_i = 0, \tag{23}$$

where Re and We are the Reynolds and Weber numbers defined as:

$$Re = \frac{U_o R}{\nu} \tag{24}$$

and

$$We = \frac{\rho U_o^2 R}{\sigma} \tag{25}$$

A second-order polynomial in η is chosen for the normalized velocity profile within the boundary layer:

$$\phi(\zeta, \eta) = 1 + \gamma_1\eta + \gamma_2\eta^2 \tag{26}$$

Equation 26 satisfies the no-slip condition at the wall. This set of equations describes the flow around the Taylor bubble.

Numerical Strategy

The constant flow rate equation, Eq. 21, and the tangential shear condition at the interface, Eq. 23, are solved for γ_1 and γ_2. Replacing γ_1 and γ_2 in the momentum integral equation, Eq. 20, leads to an expression for the pressure gradient as a function of δ and its first derivative. A third-order differential equation in δ is derived by eliminating the pressure gradient using the derivative of the normal stress condition at the interface, Eq. 22. The software Macsyma was used to develop this very long equation which has the functional form:

$$\frac{d\delta^3}{d\zeta^3} = \frac{d^3\delta}{d\zeta^3}\left[\frac{d^2\delta}{d\zeta^2}, \frac{d\delta}{d\zeta}, \delta, Re, We, \theta\right] \tag{27}$$

The integration is initiated at a position in the liquid film between the front and the back where the thickness is a minimum such as point A in Figure 2. The visual studies show that the film thickness changes very slowly near this minimum; therefore, to initiate the integration, both the first and second derivatives are assumed zero:

$$\frac{d^2\delta}{d\zeta^2}=\frac{d\delta}{d\zeta}=0. \tag{28}$$

Given a mixture velocity, U_m, the bubble velocity, U_o, and selecting an initial film thickness, δ_a such that $\delta_a>\delta_o=h_o/R$, the third-order differential equation, Eq. 27, is integrated in the forward direction from point A (Figure 2) to the front stagnation point. The interfacial velocity, $\phi_i=1+\gamma_1+\gamma_2$, is computed at each step and the integration halted when the stagnation point has been reached: that is, when $\phi_i=0$. The process is then repeated starting at A, but integrating in the reverse direction, until the rear stagnation point is reached.

These integrations provide the film thickness profile, thus the radii of curvature at each stagnation point can be computed (Eq. 16). Then, the distance from the forward stagnation point to the nose and the rear stagnation point to the furthermost rear point on the axis can be calculated, since the surface is assumed to be a sphere. From the shape it is then possible to compute the void fraction of the Taylor bubble, α_s. Many such integrations have shown that the distance from A to the rear stagnation point contributes little to the length of the bubble. In addition, the radius of the curvature at the rear is large so that the added length due to the sphere is also small. The length of the bubble is essentially determined by the forward integration.

The value of U_m required as input for this calculation is determined by the flow rates of liquid and gas. However, the Taylor bubble velocity, U_o is not known *a priori*. The requirement that the nose of the bubble must assume a spherical shape can now be used to evolve a criterion for selecting U_o. Thus, it is suggested that the experimentally observed value of U_0 is the one, for which the two radii of curvature at the nose are equal. The computed ratio of the radii of curvature at the nose is shown in Figure 5 for three values of U_o. The system is air-water slug flow in a 0.0127-m-ID tube operating at $U_m=1.0$ m/s. Over the entire possible range of initial film thickness, δ_a, only the value of $U_o=1.2$ produces unity for the ratio of the radii of curvature at the nose. This is in good agreement with the experimentally measured value of $U_o=1.22$ (Janicot, 1988). Similar results were obtained for all slug flow runs.

Typical Results

Figure 6 shows the effects of the initial film thickness on the Taylor bubble length and void fraction. Study of the films during low-gravity runs show the existence of a wide range of Taylor bubble lengths for each set of flow conditions for which slug flow existed. This suggests that the random process of bubble formation at the entrance causes different initial values of film thickness, and this results in a range of bubble lengths as shown in Figure 6.

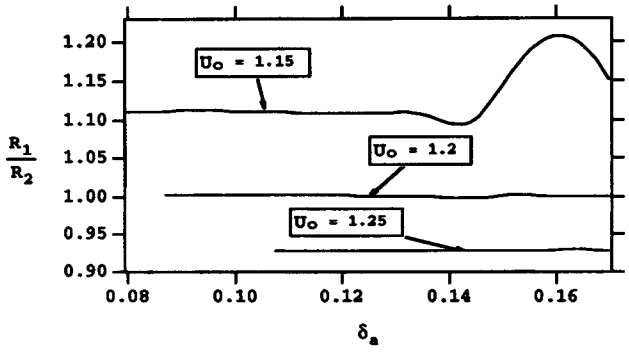

Figure 5. Effect of U_0 on the radius of curvature ratio at the nose.

Air-water at $U_m=1.0$ m/s

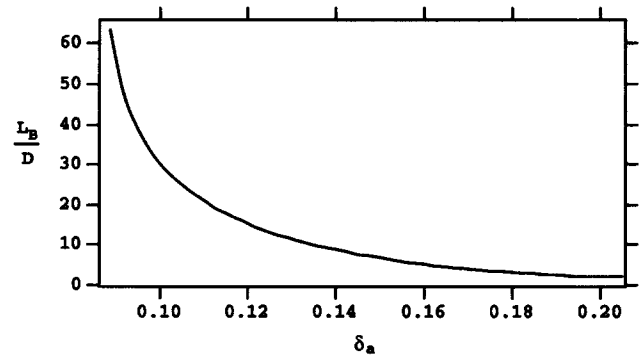

Figure 6. Effect of initial film thickness on the Taylor bubble length.

Air water with $D=0.0127$ m, $U_m=1.0$ m/s, and $U_0=1.2$ m/s.

The velocity profile constant, C_o, is defined as the ratio of the Taylor bubble velocity to the mixture velocity:

$$C_o=\frac{U_o}{U_m}. \tag{29}$$

This quantity has been widely used to characterize slug flow. The Taylor bubble velocity computed by the procedures described above is shown in terms of C_o in Figure 7.

Closure Relationships and Solution Procedure

A full description of slug flow under reduced gravity conditions would provide the length, L_B, and shape of the Taylor bubble (thus the bubble void fraction, α_B), the length of the liquid slug, L_s, its void fraction, σ_S, and the velocity of propagation of the slugs and bubbles, U_o. The discussion above provides the method to compute U_o, L_B, and α_B. Given the frequency of slugging, ν_s, and the void fraction in the liquid slugs, α_s, the remaining quantities can be computed as shown below.

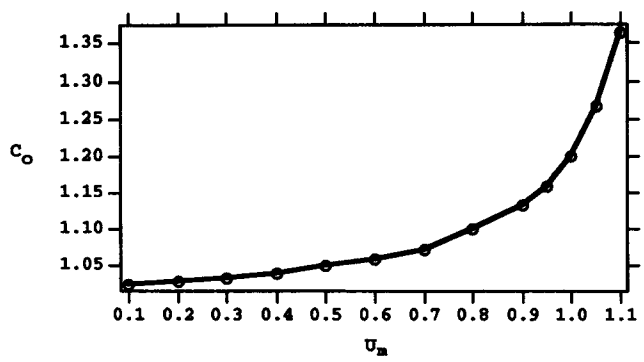

Figure 7. Velocity profile constant, C_0.

Combining Eqs. 10 and 11 from the material balance network yields:

$$U_{SG}=(1-\beta)\alpha_s U_o+\beta\alpha_B U_o \tag{30}$$

The definition of slug frequency provides the following relationship:

$$\nu_s=\frac{U_o}{[L_s+L_B]}=\frac{U_0\beta}{L_B} \tag{31}$$

For the limiting case when the slugs are voids free ($\alpha_s\rightarrow 0$) Eqs. 30 and 31 can be combined to give:

$$U_G=\nu_s L_B\alpha_B \tag{32}$$

Then, the calculation proceeds by assuming values of δ_a and U_o and integrating along the bubble as discussed above to obtain L_B, α_B and the value of U_o which results in a spherical nose. The process is repeated varying δ_α until values are obtained which satisfy Eq. 32. Then, the slug length, L_s, can be computed from Eq. 31.

For nonzero values of α_s, the procedure is only slightly more involved. Select initial values of δ_a and U_o, and compute L_B, α_B and the value of U_0 which produces the spherical nose. Use Eq. 31 to calculate β and check to see if Eq. 30 is satisfied. If not, assume a new set of initial values and iterate.

The need to specify the slugging frequency and slug void fraction to obtain closure in the model is exactly equivalent to the situation which exists in models developed for 1 g, as discussed above. Studies by Janicot (1988) indicate that the slug void fraction is also controlled by the mixer characteristics. However, at this point, models for these quantities have yet to be developed.

Conclusion and Significance

A new physical model has been constructed describing steady gas-liquid slug flow at reduced gravity. Insights derived from experimental observations suggested the use of a boundary layer approach. A third-order differential equation was developed which could be used to compute the bubble length and shape, and a method for computing the velocity was presented. A procedure was proposed from which the slug length could be calculated.

Notation

D = tube diameter
h = local thickness of film surrounding Taylor bubble
L_B = Taylor bubble length
L_s = slug length
p = static pressure
r = radial coordinate
R = tube radius
R_1, R_2 = radii of curvature
Re = Reynolds number (Eq. 24)
u = local axial velocity
U_B = gas velocity in the Taylor bubble
U_{DL} = drift velocity of liquid (Eq. 3)
U_{DG} = drift velocity of gas (Eq. 4)
U_f = liquid velocity in film surrounding the Taylor bubble
U_G = gas velocity in the liquid slug
U_m = superficial mixture velocity, $U_{SL}+U_{SG}$
U_o = propagation velocity of the Taylor bubble
U_s = liquid velocity in the slug
U_{SG} = superficial gas velocity
U_{SL} = superficial liquid velocity
We = Weber number (Eq. 25)
z = axial coordinate

Greek letters

α_B = void fraction over length of the Taylor bubble
α_s = void fraction in the liquid slug
α_{SU} = void fraction of the slug unit
β = $L_B/(L_S+L_B)$
δ = dimensionless film thickness (Eq. 19)
δ_a = initial film thickness used in integration
δ_0 = minimum film thickness for liquid film at rest
ζ = dimensionless axial distance (Eq. 19)
η = dimensionless radial distance (Eq. 19)
θ = dimensionless mixture velocity (Eq. 19)
λ = dimensionless pressure gradient (Eq. 19)
ν = kinematic viscosity
ρ = liquid density
σ = surface tension
ϕ = dimensionless velocity (Eq. 19)

Literature Cited

Bendiksen, K. H., "On the Motion of Long Bubbles in Vertical Tubes," *Int. J. Multiphase Flow*, **11**, 797 (1985).

Bretherton, F. P., "The Motion of Long Bubbles in Tubes," *J. Fluid Mech.*, **175**, 557 (1987).

Collins, R., F. F. De Morales, J. F. Davidson, and D. Harisson, "The Motion of a Large Gas Bubble Rising Through Liquid Flowing in a Tube," *J. Fluid Mech.*, **89**, 497 (1978).

Coney, T., and W. J. Masica, "The Effect of Flow Rate on the Dynamic Contact Angle for Wetting Liquids," NASA TN D-5115 (1969).

Davies, R. M., and G. Taylor, "The Mechanics of Large Bubbles Rising Through Extended Liquids and Through Liquids in Tubes," *Proc. Roy. Soc. Ser. A*, **200**, 375 (1950).

Dukler, A. E., J. A. Fabre, J. B. McQuillen, and R. Vernon, "Gas Liquid Flow at Microgravity Conditions: Flow Patterns and Their Transitions," *Int. J. Multiphase Flow*, **14**, 389 (1988).

Dukler, A. E., and M. G. Hubbard, "A Model for Slug Flow in Horizontal and Near Horizontal Tubes," *Ind. Eng. Chem. Fund.*, **14**, 337 (1975).

Dumitrescu, D. T., "Stromung an Einer Luftblase im Senkrechten Rohr," *Z. Angew. Math. Mech.*, **23**, 139 (1943).

Fernandes, R., R. Semiat, and A. E. Dukler, "A Hydrodynamic Model for Gas-Liquid Slug Flow in Vertical Tubes," *AIChE J.*, **26**, 337 (1983).

Janicot, A., "Studies of Gas-Liquid Flow Under Reduced Gravity Conditions," MS Thesis, Univ. of Houston (1988).

Mao, Z., and A. E. Dukler, "The Motion of Taylor Bubbles in Vertical Tubes: I. A Numerical Simulation for the Shape and Rise Velocity of Taylor Bubbles in Stagnant and Flowing Liquid," *J. Comp. Phys.*, **91**, 132 (1990).

Reinelt, D. A., "The Rate at Which a Long Bubble Rises in a Vertical Tube," *J. Fluid Mech.*, **175**, 557 (1987).

Taitel, Y., and A. E. Dukler, "A Model for Slug Frequency during Gas Liquid Flow in Horizontal and Near Horizontal Tubes," *Omt. J. Mult. Flow*, **3**, 585 (1977).

Tronconi, E., "Prediction of Slug Frequency in Horizontal Two-Phase Slug Flow," *AIChE J.*, **36**, 701 (1990).

Manuscript received Nov. 5, 1991, and revision received Dec. 2, 1992.